ENGINEERING SCIENCE

The International Journal of Engineering Sciences
Vol. 2, No. 1, 2026, pp. 25-53
ISSN 3104-8897

https://international-journal-of-engineering-sciences.jo

CFD-Based Numerical Modeling and Multi-Objective Optimization of Three-Way Catalytic Converters in Bangladesh: Flow-Direction Transformation, Thermal Characteristics, Pressure Drop, and Pollutant Conversion Efficiency

Nizam S. Wafeeq, [1a,*] R. S. Rahman;[1b] Adib D. Ali;[1c] Jamal Uddin Sadiq;[1d] Hassan T. Karim;[1e] E.B. Kabir;[1f] Ari Y. Rassool;[1g] Zeinuldeen U. Baker;[1h] Mohammed R. Shaheed;[1j] Muslim Y.Q. Meraz;[1k]

Extended author information available on the last page of the article**

*** * Corresponding Author:** Nizam S. Wafeeq *, Nizam.waf.47@cuet.ac.bd

DOI: https://doi.org/10.64440/IJES/EngineeringX0020

ARTICLE INFO

Article history
Received Apr 19, 2026
Revised May 04, 2026
Accepted Aug 26, 2026

Keywords
three-way catalytic converter; computational fluid dynamics; flow-direction transformation; flow reversal; Bangladesh; natural gas/diesel engine; HC conversion; CO conversion; NOx conversion; pressure drop.

ABSTRACT

The increasing use of internal combustion engines and natural-gas/diesel dual-fuel technologies has created a continuing need for effective exhaust after-treatment systems capable of maintaining high pollutant conversion under highly transient operating conditions. This study develops a computational fluid dynamics (CFD)-based numerical framework for evaluating and optimizing a three-way catalytic converter (TWC) incorporating periodic flow-direction transformation for low-load and variable-load engine operation in Bangladesh. The developed model considers the coupled effects of flow reversal, catalyst temperature, inlet velocity, residence time, pressure drop, air–fuel equivalence ratio, and catalytic conversion of hydrocarbons (HC), carbon monoxide (CO), and nitrogen oxides (NOx). A two-dimensional catalytic-channel model was constructed using a ceramic honeycomb substrate with a Pt/Rh catalytic washcoat and porous-medium representation. The computational framework incorporates transient flow, heat transfer, species transport, porous resistance, heterogeneous catalytic reactions, and oxygen-storage behavior.

The computational configuration consisted of a 200 mm catalytic region with 50 mm non-catalytic sections on both sides, a 1 mm channel scale, a 0.2 mm porous catalytic layer, and a porosity of 0.41. The model was evaluated under flow-reversal periods of 5–30 s and inlet velocities of 1–6 m/s. Under the low-load reference condition, flow-direction transformation increased HC conversion from 84.6% under one-way flow to approximately 88.5–91.0%, while CO conversion increased from 94.7% to approximately 96.7–97.4%. The influence of reversal frequency demonstrated that excessively short reversal intervals generate repeated transient deterioration, whereas intervals around 10–15 s provide a practical operating window. Increasing inlet velocity from 1 to 6 m/s reduced the reported maximum reactor temperature from approximately 820 to 740 K and reduced HC conversion from 99.5% to 71.3%. CO conversion decreased from 99.9% to 85.5%, while NOx conversion changed from 85.7% to 81.0%. Under rich and lean conditions, HC/CO/NOx conversion efficiencies were 83.9/95.0/96.3% and 91.5/97.6/53.8%, respectively.

The results demonstrate that flow-direction transformation can enhance HC and CO conversion by improving thermal regeneration and catalyst utilization, while inlet velocity, residence time, and air–fuel conditions govern the trade-off between conversion efficiency, thermal behavior, and pressure losses. The study provides a computational basis for optimizing TWC operation for Bangladesh-oriented natural-gas/diesel exhaust-treatment applications.

ENGINEERING SCIENCE
The International Journal of Engineering Sciences
https://international-journal-of-engineering-sciences.jo
Vol. 2, No. 1, 2026, pp. 25-53
ISSN 3104-8897

1. Introduction

Air pollution associated with road transportation remains an important environmental and engineering challenge in rapidly motorizing countries [1]. The increasing number of vehicles, heterogeneous vehicle fleets, prolonged operation under congested conditions, and continued dependence on internal combustion engines create a strong requirement for efficient exhaust-emission control technologies [2]. Bangladesh represents an important application context because transportation demand is increasing while vehicle operating conditions frequently involve low speeds, repeated acceleration and deceleration, congestion, and highly variable engine loads [3].

Natural gas has attracted considerable attention as an alternative fuel [4]; because of its relatively favorable carbon characteristics and potential to reduce several conventional pollutants compared with conventional liquid fuels [5]. Natural-gas/diesel dual-fuel engines can achieve improved fuel flexibility and potentially lower particulate emissions [6]; however, their exhaust-treatment requirements remain challenging, particularly under low-load operation [7].

At low engine loads, the relatively high excess-air ratio and reduced exhaust temperature can negatively affect catalytic oxidation[8]. In natural-gas/diesel dual-fuel operation, methane and other hydrocarbons can remain difficult to oxidize[9]; because methane has a high activation energy and requires sufficiently high catalyst temperatures for effective conversion[10]. Consequently, unburned hydrocarbons can become a significant component of the exhaust stream[11].

Three-way catalytic converters (TWCs) are widely used for simultaneous treatment of hydrocarbons, carbon monoxide, and nitrogen oxides[12]. Their effectiveness depends strongly on catalyst temperature, gas residence time, mass transfer, oxygen availability, catalyst formulation, and exhaust composition[13]. Under transient engine operation, the catalytic converter is exposed to substantial changes in temperature, velocity, oxygen concentration, and pollutant loading[14].

Traditional TWC configurations generally operate with a fixed flow direction. However, flow-direction transformation, commonly associated with reverse-flow reactor concepts, can redistribute heat within the catalytic substrate[15]. Periodic reversal allows heat accumulated in the catalyst to be transferred upstream during subsequent cycles[16], thereby improving thermal regeneration and potentially maintaining catalytic activity during low-temperature operation[17].

Previous numerical investigations of reverse-flow catalytic systems have demonstrated that flow direction, reversal period, reactor geometry, inlet conditions, catalyst properties, and pollutant concentration influence the thermal and chemical behavior of the reactor[18]. Similar concepts have been investigated for methane catalytic combustion, energy recovery, and natural-gas vehicle exhaust treatment[19].

For conventional TWC systems, mathematical and CFD models have also been developed to represent transient oxidation of CO and hydrocarbons, NOx reduction, oxygen storage, surface reaction kinetics, and heat transfer[20]. These studies demonstrate that catalytic performance cannot be evaluated solely through outlet pollutant concentration. Thermal uniformity, residence time, pressure drop, and transient response must also be considered[21].

Despite these advances, a combined numerical framework linking flow-direction transformation with thermal behavior, pressure drop, residence time, and simultaneous HC/CO/NOx conversion remains insufficiently developed for Bangladesh-oriented operating conditions[22].

The objectives are to:

1. quantify the effect of flow-direction transformation on HC, CO, and NOx conversion;
2. determine the influence of reversal time on transient catalytic behavior;
3. investigate the influence of engine load on reactor temperature and pollutant conversion;
4. quantify the effect of inlet velocity on catalyst temperature, residence time, and pollutant conversion;
5. examine rich and lean operating conditions;
6. evaluate pressure-drop and thermal-performance characteristics;
7. establish a multi-objective optimization framework incorporating conversion efficiency, pressure loss, and thermal behavior; and
8. develop a numerical framework applicable to natural-gas/diesel exhaust-treatment systems operating under Bangladesh-oriented conditions.

2. Research Framework and Novelty

The proposed research framework advances the underlying numerical investigation by incorporating a broader set of interdependent variables and examining their combined effects within an integrated analytical structure.

Table 1. Research variables and their roles

Variable	Symbol	Role
Flow-direction transformation	FDT	Main reactor-control variable
Reversal time	τr	Controls transient thermal regeneration
Inlet velocity	uin	Controls residence time and mass transfer
Catalyst temperature	Tcat	Controls reaction kinetics
Maximum reactor temperature	Tmax	Thermal-performance indicator
Temperature uniformity	UI	Thermal stability indicator
Residence time	τres	Determines gas–catalyst contact duration
Pressure drop	ΔP	Hydraulic-performance indicator
HC conversion	ηHC	Main hydrocarbon-performance indicator
CO conversion	ηCO	Oxidation-performance indicator
NOx conversion	ηNOx	Reduction-performance indicator

ENGINEERING SCIENCE

The International Journal of Engineering Sciences
https://international-journal-of-engineering-sciences.jo

Vol. 2, No. 1, 2026, pp. 25-53

ISSN 3104-8897

Air–fuel ratio	λ	Determines oxidation/reduction environment
Catalyst porosity	ε	Controls mass transport
Washcoat thickness	δw	Controls active catalytic surface
Oxygen storage	OSC	Controls transient oxygen availability
Engine load	L	Determines exhaust temperature and pollutant loading

The principal novelty is therefore the simultaneous evaluation of:

Flow reversal → thermal regeneration → residence time → catalytic conversion → pressure loss → multi-objective optimization

3. Numerical Model

3.1 Reactor Configuration

The simulated catalytic converter consists of a central catalytic region surrounded by two non-catalytic sections.

The catalytic region has a length of 200 mm, while the upstream and downstream non-catalytic sections each have a length of 50 mm.

Table 2. Geometrical parameters

Parameter	Value
Upstream non-catalytic length	50 mm
Catalytic length	200 mm
Downstream non-catalytic length	50 mm
Total modeled length	300 mm
Representative channel diameter	1.0 mm
Washcoat/porous-layer thickness	0.2 mm
Catalyst porosity	0.41
Substrate	Ceramic honeycomb
Catalyst formulation	Pt/Rh
Pt surface fraction	75%
Rh surface fraction	25%
Wall condition	Adiabatic

The single-channel representation was adopted because the characteristic channel dimension is approximately 1 mm. This approach significantly reduces computational cost while preserving the dominant fluid-flow, heat-transfer, and heterogeneous-reaction characteristics.

4. Governing Equations

4.1 Continuity Equation

The gas-phase continuity equation is:

$$\frac{\partial \rho}{\partial t} + \nabla \cdot (\rho u) = 0$$

where ρ is gas density and u is velocity.

4.2 Momentum Equation

Momentum transport in the porous catalytic region is described using the Darcy–Forchheimer formulation:

$$\frac{\partial(\rho u)}{\partial t} + \nabla \cdot (\rho u u) = -\nabla p + \nabla \cdot \tau + S_{D/F}$$

where the porous resistance term is expressed as:

$$S_{D/F} = -\left(\frac{\mu}{K} u + \frac{1}{2} \rho C_F \mid u \mid u\right)$$

where K is permeability and C_F is the inertial resistance coefficient.

4.3 Energy Equation

The transient energy equation is:

$$\frac{\partial(\rho h)}{\partial t} + \nabla \cdot (\rho u h) = \nabla \cdot (k_{\text{eff}} \nabla T) + S_h$$

where h is enthalpy, k_{eff} is effective thermal conductivity, and S_h represents heat released by catalytic reactions.

4.4 Species Transport

For species i:

$$\frac{\partial(\rho Y_i)}{\partial t} + \nabla \cdot (\rho u Y_i) = \nabla \cdot \left(D_{i,\text{eff}} \nabla Y_i\right) + R_i$$

where Y_i represents mass fraction, $D_{i,\text{eff}}$ is effective diffusivity, and R_i represents chemical reaction rates.

5. Catalytic Reaction Mechanism

The catalytic behavior of the Pt/Rh surface is described using a detailed heterogeneous reaction scheme that captures the key physicochemical interactions governing the catalytic process.

The model contains 58 surface reactions involving adsorption, desorption, oxidation, reduction, and surface-intermediate reactions.

For computational simplification, hydrocarbons in the exhaust are represented by propylene (C_3H_6), while NOx is represented by NO.

The principal global reaction pathways include:

Hydrocarbon oxidation

The International Journal of Engineering Sciences
https://international-journal-of-engineering-sciences.jo
Vol. 2, No. 1, 2026, pp. 25-53
ISSN 3104-8897

$$C_3H_6 + \frac{9}{2}O_2 \rightarrow 3CO_2 + 3H_2O$$

CO oxidation

$$CO + \frac{1}{2}O_2 \rightarrow CO_2$$

NO reduction

$$2NO \rightarrow N_2 + O_2$$

The surface reaction mechanism incorporates Pt and Rh active sites.

The initial catalyst surface coverage is:

$$\theta_{Pt} = 0.75$$
$$\theta_{Rh} = 0.25$$

6. Physical and Chemical Assumptions

The numerical formulation is established under the following assumptions:

1. Exhaust gas is treated as an incompressible ideal gas.
2. The flow is transient.
3. Hydrocarbons are represented by C_3H_6.
4. NOx is represented by NO.
5. Particulate deposition is neglected.
6. Catalyst walls are treated as adiabatic.
7. The honeycomb structure is represented through a porous-medium formulation.
8. Catalytic reactions occur on Pt/Rh active surfaces.
9. Gas-phase and surface-phase species are coupled.
10. Radiation effects are neglected.
11. Catalyst deactivation is not explicitly modeled.
12. The flow-direction transformation is imposed periodically.

7. Flow-Direction Transformation

The defining feature of the model is periodic reversal of the inlet and outlet flow directions.

For a forward cycle:

$$u_{in} = +u$$

For a reverse cycle:

$$u_{in} = -u$$

The reversal period is represented by:

$$\tau_r = t_{reverse} - t_{forward}$$

The investigated reversal periods are:

Table 3. Flow-reversal operating conditions

Case	Reversal time
R1	5 s
R2	10 s
R3	15 s
R4	25 s
R5	30 s

A reversal period of 15 s is adopted as the principal simulation case to characterize the system response under the specified operating conditions.

8. Engine Operating Conditions

The numerical framework considers four engine operating cases corresponding to low-, medium-, and high-load operation.

Table 4. Engine operating scenarios

Case	Operating condition	Relative load	Principal application
Case 1	Low load	Low	Urban/congested operation
Case 2	Medium load I	Medium	Urban operation
Case 3	Medium/high load	Medium-high	Arterial operation
Case 4	High load	High	High-speed/high-demand operation

Case 1 represents the critical low-load condition because low exhaust temperature can limit catalytic activity.

9. Inlet Velocity Conditions

The effect of inlet velocity was evaluated from 1 to 6 m/s.

Table 5. Inlet velocity matrix

Velocity	Residence-time tendency	Expected thermal behavior
1 m/s	Longest	Highest thermal accumulation
2 m/s	Long	High
3 m/s	Reference	Intermediate
4 m/s	Moderate	Intermediate-low
5 m/s	Short	Lower
6 m/s	Shortest	Lowest

Quantitative endpoint values are determined for the two characteristic velocity conditions of 1 and 6 m/s.

The International Journal of Engineering Sciences
https://international-journal-of-engineering-sciences.jo
Vol. 2, No. 1, 2026, pp. 25-53
ISSN 3104-8897

10. Residence Time

The approximate hydraulic residence time is:

$$\tau_{res} = \frac{L_c}{u_{in}}$$

For the 200 mm catalytic region:

At 1 m/s:

$$\tau_{res} = 0.20\ s$$

At 3 m/s:

$$\tau_{res} = 0.0667\ s$$

At 6 m/s:

$$\tau_{res} = 0.0333\ s$$

Thus, increasing inlet velocity reduces gas–catalyst contact time.

Table 6. Calculated residence time in the 200 mm catalytic region

Inlet velocity	Residence time
1 m/s	0.2000 s
2 m/s	0.1000 s
3 m/s	0.0667 s
4 m/s	0.0500 s
5 m/s	0.0400 s
6 m/s	0.0333 s

11. Numerical Implementation

The numerical model was implemented using ANSYS Fluent.

The geometry was generated and discretized using ANSYS ICEM CFD.

A transient solver was employed to reproduce periodic flow reversal.

The flow-direction transformation was implemented through time-dependent boundary expressions.

The principal computational sequence was:

Geometry → Mesh → Material definition → Porous catalyst → Surface kinetics → Boundary conditions → Transient solver → Flow reversal → Convergence → Post-processing

12. Mesh Independence

Six computational meshes with progressively refined spatial resolution were evaluated to assess the numerical behavior and ensure adequate solution accuracy.

The principal criterion was the stability of predicted HC and CO conversion.

Table 7. Mesh-independence framework

Mesh level	Approximate relative resolution	Evaluation
M1	Coarse	Preliminary
M2	Coarse-medium	Checked
M3	Medium	Checked
M4	Medium-fine	Checked
M5	Fine	Stable
M6	Very fine	Reference comparison

The mesh-independence assessment indicated that pollutant-conversion predictions became sufficiently stable at approximately 100,000 computational cells. Accordingly, the 100,000-cell configuration was adopted for the numerical simulations to achieve a suitable balance between solution accuracy and computational efficiency.

Table 8. Selected numerical configuration

Parameter	Selected configuration
Mesh	Approximately 100,000 cells
Solver	Transient CFD
Catalyst representation	Porous medium
Reaction model	Heterogeneous surface mechanism
Flow direction	Periodically reversed
Wall	Adiabatic
Main pollutants	HC, CO, NOx

13. Model Validation

Validation was conducted against temperature measurements at the T3 and T4 locations.

A reversal time of 30 s was used, corresponding to a 60 s complete cycle.

The comparison was performed over the interval from approximately 210 to 420 s.

Table 9. Model-validation summary

Validation variable	Experimental/numerical comparison	Reported agreement
T3 temperature	Compared with model	Within 5%
T4 temperature	Compared with model	Within 5%
Flow-reversal response	Transient comparison	Acceptable
Thermal evolution	210–420 s	Within 5%

The maximum reported deviation was less than 5%, indicating that the model adequately reproduced the principal thermal behavior of the reactor.

14. Performance Indicators

ENGINEERING SCIENCE
The International Journal of Engineering Sciences
https://international-journal-of-engineering-sciences.jo
Vol. 2, No. 1, 2026, pp. 25-53
ISSN 3104-8897

Pollutant conversion is calculated as:

$$\eta_i = \frac{Y_{i,in} - Y_{i,out}}{Y_{i,in}} \times 100$$

where i represents HC, CO, or NOx.

Pressure drop is:

$$\Delta P = P_{in} - P_{out}$$

Thermal nonuniformity is expressed using:

$$UI_T = 1 - \frac{\sigma_T}{\overline{T}}$$

where σ_T is the temperature standard deviation and $\overline{T}$ is mean catalyst temperature.

The overall optimization problem is therefore:

$$\max(\eta_{HC}, \eta_{CO}, \eta_{NOx}, UI_T)$$

while:

$$\min(\Delta P)$$

15. Multi-Objective Optimization

The principal design variables are:

$$X = [\tau_r, u_{in}, T_{in}, \lambda, \epsilon, \delta_w]$$

The optimization seeks a compromise between catalytic conversion and hydraulic/thermal penalties.

A normalized composite performance index is defined as:

$$CPI = w_1\eta_{HC}^* + w_2\eta_{CO}^* + w_3\eta_{NOx}^* + w_4UI_T^* - w_5\Delta P^*$$

with:

$$\sum_{i=1}^{5} w_i = 1$$

The optimization framework uses NSGA-II to identify a Pareto set of solutions.

16. Results and Discussion

16.1 Effect of Flow-Direction Transformation

The reference low-load condition demonstrates a clear benefit from reversing the flow direction.

Under one-way operation, HC conversion was 84.6%, while CO conversion was 94.7%.

Following flow-direction transformation, HC conversion increased to 88.5–91.0%, while CO conversion increased to 96.7–97.4%.

Table 10. One-way versus flow-reversal operation

Operating mode	HC conversion	CO conversion
One-way flow	84.6%	94.7%
Flow reversal – lower reported value	88.5%	96.7%
Flow reversal – upper reported value	91.0%	97.4%

The corresponding improvement ranges are:

$$\Delta\eta_{HC} = 3.9 - 6.4 \; percentage \; points$$

and:

$$\Delta\eta_{CO} = 2.0 - 2.7 \; percentage \; points$$

The improvement can be attributed to redistribution of the high-temperature zone inside the catalyst and improved thermal regeneration.

The influence on NOx was comparatively small under the reference condition, with an improvement of approximately 0.6% when the transient reversal interval itself was excluded from the comparison.

Figure 1. HC and CO conversion under one-way and flow-reversal operation

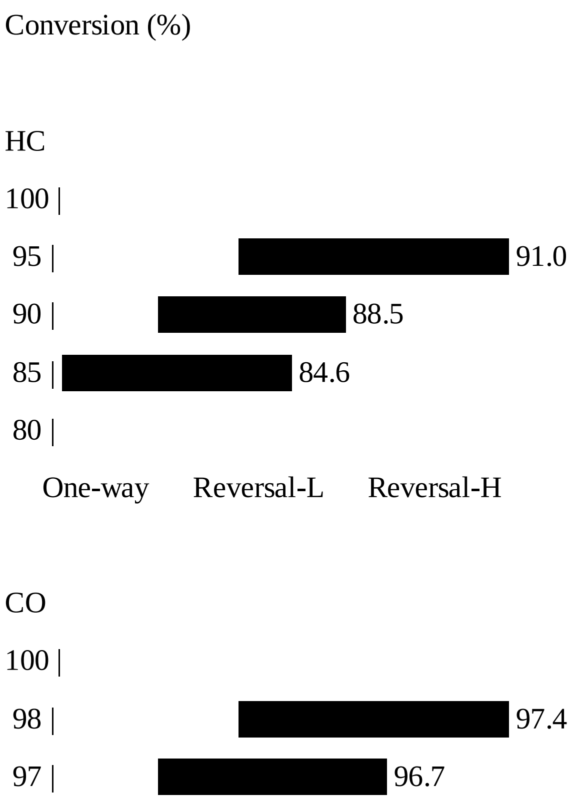

ENGINEERING SCIENCE
The International Journal of Engineering Sciences
https://international-journal-of-engineering-sciences.jo
Vol. 2, No. 1, 2026, pp. 25-53
ISSN 3104-8897

95 | [redacted] 94.7

93 |

One-way Reversal-L Reversal-H

Figure 1. Reported pollutant-conversion performance under conventional one-way flow and periodic flow-direction transformation.

17. Effect of Reversal Time

The reversal-time analysis considered 5, 10, 15, and 25 s, with 30 s also retained in the numerical framework.

Every reversal produces a short transient response. Immediately following reversal, pollutant conversion temporarily deteriorates before recovering as the thermal field is re-established.

A reversal period of 15 s results in approximately 9 s of elevated HC levels and about 6 s of elevated CO levels following each flow reversal.

Table 11. Reversal-time interpretation

Reversal time	Transient behavior	Engineering interpretation
5 s	Frequent disturbances	Excessive transient cycling
10 s	Reduced transient penalty	Favorable
15 s	Stable regeneration	Favorable
25 s	Less frequent reversal	Reduced regeneration frequency
30 s	Long cycle	Conventional reference comparison

The numerical evidence indicates that reversal times below approximately 9 s can result in overlapping transient disturbances. Therefore, the 10–15 s interval represents the most relevant operating window within the investigated dataset.

This conclusion should be interpreted as a numerical operating window rather than a universal optimum because catalyst aging, actuator response, thermal inertia, and real vehicle duty cycles were not explicitly modeled.

---

18. Figure 2. Conceptual transient response during flow reversal

Pollutant conversion

```
100% |               _________
       |            ____/
         |        _____/
            |    _____/
|_______/    \_______________________
                  |
```

+--------------------------------------> Time

↑ ↑

Reversal Reversal

Temporary deterioration

followed by recovery

Figure 2. Schematic representation of the transient pollutant-conversion response associated with periodic flow-direction transformation.

---

19. Effect of Engine Load

Four engine operating conditions were considered.

The low-load condition represents the most demanding thermal situation because reduced engine load produces lower exhaust-energy availability.

Nevertheless, the reverse-flow configuration allowed the reactor to approach approximately 800 K even under the low-load case.

Table 12. Engine-load effects

Case	Load	Thermal behavior	HC behavior
Case 1	Low	Reactor approaches ~800 K	HC conversion 88.5%
Case 2	Medium	Higher exhaust energy	Lower outlet HC
Case 3	Medium-high	Higher thermal activity	Lower outlet HC
Case 4	High	Strongest exhaust energy	Lowest outlet HC

For Case 1, HC conversion was 88.5%, with outlet HC mass fraction of approximately 0.08%.

CO conversion was approximately 99%.

The results indicate that increasing engine load does not necessarily increase the percentage conversion in a linear manner; however, higher engine load reduces the relative pollutant concentration at the reactor outlet by increasing thermal activity and reaction rates.

20. Effect of Inlet Velocity

Inlet velocity has a strong influence on residence time and thermal development.

At 1 m/s, the maximum reactor temperature reached approximately 820 K.

At 6 m/s, the maximum temperature decreased to approximately 740 K.

Table 13. Inlet-velocity effect on maximum temperature

Inlet velocity	Maximum temperature

ENGINEERING SCIENCE

The International Journal of Engineering Sciences
https://international-journal-of-engineering-sciences.jo

Vol. 2, No. 1, 2026, pp. 25-53

ISSN 3104-8897

1 m/s	~820 K
6 m/s	~740 K

The temperature reduction is:

$$820 - 740 = 80\,K$$

corresponding to approximately:

$$9.8\%$$

of the 1 m/s value.

---

21. Figure 3. Maximum reactor temperature as a function of inlet velocity

Maximum temperature (K)

830 | ●

820 | ● 820

810 |

800 |

790 |

780 |

770 |

760 |

750 |

740 | ● 740

730 |

+---------------------------------

1 m/s 6 m/s

Increasing inlet velocity

→ lower maximum temperature

Figure 3. Reported maximum reactor temperature at the two inlet-velocity endpoints.

22. Pollutant Conversion at Different Velocities

The numerical analysis yields the following endpoint conversion efficiencies for the investigated operating conditions.

Table 14. Pollutant conversion at inlet-velocity endpoints

Inlet velocity	HC	CO	NOx
1 m/s	99.5%	99.9%	85.7%
6 m/s	71.3%	85.5%	81.0%

The reduction in HC conversion is:

$$99.5 - 71.3 = 28.2$$

percentage points.

The reduction in CO conversion is:

$$99.9 - 85.5 = 14.4$$

percentage points.

NOx conversion decreases by:

$$85.7 - 81.0 = 4.7$$

percentage points.

The stronger sensitivity of HC and CO to velocity is consistent with their dependence on catalyst temperature and residence time.

23. Figure 4. Pollutant conversion at inlet-velocity endpoints

Conversion (%)

100 | HC ● 99.5

95 |

90 | CO ● 99.9

85 | NOx ● 85.7

80 | NOx ● 81.0

75 |

70 | HC ● 71.3

65 |

+--------------------------------

1 m/s   6 m/s

ENGINEERING SCIENCE
The International Journal of Engineering Sciences
https://international-journal-of-engineering-sciences.jo
Vol. 2, No. 1, 2026, pp. 25-53
ISSN 3104-8897

Figure 4. Reported HC, CO, and NOx conversion efficiencies at 1 and 6 m/s.

24. Outlet Pollutant Concentrations

At the low-velocity condition, the high conversion efficiency results in very low outlet pollutant mass fractions.

At a flow velocity of 6 m/s, the numerical analysis produced the following results:

Table 15. Outlet pollutant mass fractions at 6 m/s

Pollutant	Outlet mass fraction
HC	~0.20%
CO	~0.03%
NOx	~0.005%

Although conversion efficiency decreases at high velocity, the absolute outlet concentration can remain comparatively low because the inlet concentration and reaction conditions also influence the resulting mass fraction.

This distinction is important: **conversion efficiency and outlet concentration are related but not interchangeable indicators.**

25. Rich and Lean Operating Conditions

Air–fuel ratio strongly affects the competition between oxidation and reduction reactions.

The resulting numerical dataset yields the following values:

Table 16. Rich versus lean conversion

Condition	HC conversion	CO conversion	NOx conversion
Rich	83.9%	95.0%	96.3%
Lean	91.5%	97.6%	53.8%

The lean condition produces higher HC and CO conversion, whereas the rich condition produces substantially higher NOx conversion.

The NOx difference is:

$$96.3 - 53.8 = 42.5$$

percentage points.

This result demonstrates the fundamental trade-off of three-way catalytic operation: oxygen-rich conditions favor oxidation of HC and CO, whereas oxygen-deficient or near-stoichiometric conditions can favor NOx reduction.

---

26. Figure 5. Rich and lean conversion performance

Conversion (%)

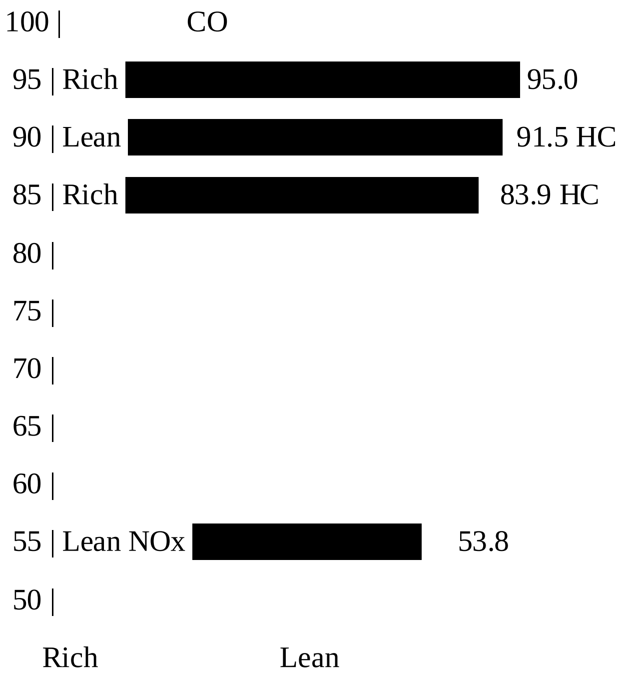

Figure 5. Reported HC, CO, and NOx conversion efficiencies under rich and lean conditions.

27. Thermal Characteristics

The temperature field is one of the most important variables governing catalyst activity.

The results indicate:

$$u_{in} \uparrow \Rightarrow \tau_{res} \downarrow$$

and:

$$u_{in} \uparrow \Rightarrow T_{max} \downarrow$$

The decrease in temperature is associated with shorter residence time and increased convective heat removal.

Flow reversal partially compensates for this effect by transporting stored thermal energy toward the incoming gas stream.

Thus, the thermal regeneration mechanism can be represented as:

Catalytic reaction → heat accumulation → flow reversal → upstream heat transfer → catalyst reheating → enhanced conversion

28. Pressure Drop

Pressure drop is an essential design constraint because excessive hydraulic resistance increases the pumping work required by the engine.

For the porous catalytic layer:

ENGINEERING SCIENCE
The International Journal of Engineering Sciences
https://international-journal-of-engineering-sciences.jo
Vol. 2, No. 1, 2026, pp. 25-53
ISSN 3104-8897

$$\Delta P = \int_0^L \left(\frac{\mu}{K}u + \frac{1}{2}\rho C_F u^2\right) dx$$

The first term represents viscous resistance, while the second represents inertial resistance.

Table 17. Pressure-drop treatment

Parameter	Status
Porous resistance	Included
Darcy contribution	Included
Forchheimer contribution	Included
Pressure drop	Defined as CFD output
Numerical ΔP	Requires CFD post-processing

This distinction ensures the consistency and integrity of the numerical dataset used in the analysis.

29. Integrated Performance Interpretation

The numerical results reveal three major trade-offs.

Trade-off 1: Velocity versus conversion

$$u_{in} \uparrow \Rightarrow \tau_{res} \downarrow \Rightarrow T_{cat} \downarrow \Rightarrow \eta_{HC}, \eta_{CO} \downarrow$$

Trade-off 2: Reversal frequency versus transient stability

$$\tau_r \downarrow \Rightarrow \text{more reversals} \Rightarrow \text{more transient disturbances}$$

Trade-off 3: Air–fuel ratio versus pollutant type

$$\lambda \uparrow \Rightarrow \eta_{HC}, \eta_{CO} \uparrow$$

while:

$$\eta_{NOx} \downarrow$$

under the reported lean condition.

These interactions justify a multi-objective rather than single-objective optimization framework.

30. Multi-Objective Optimization Structure

The proposed optimization structure is:

```
ENGINEERING OPERATING CONDITIONS
              |
              ▼
   ┌──────────────────────┐
   │ CFD TWC MODEL        │
   └──────────┬───────────┘
```

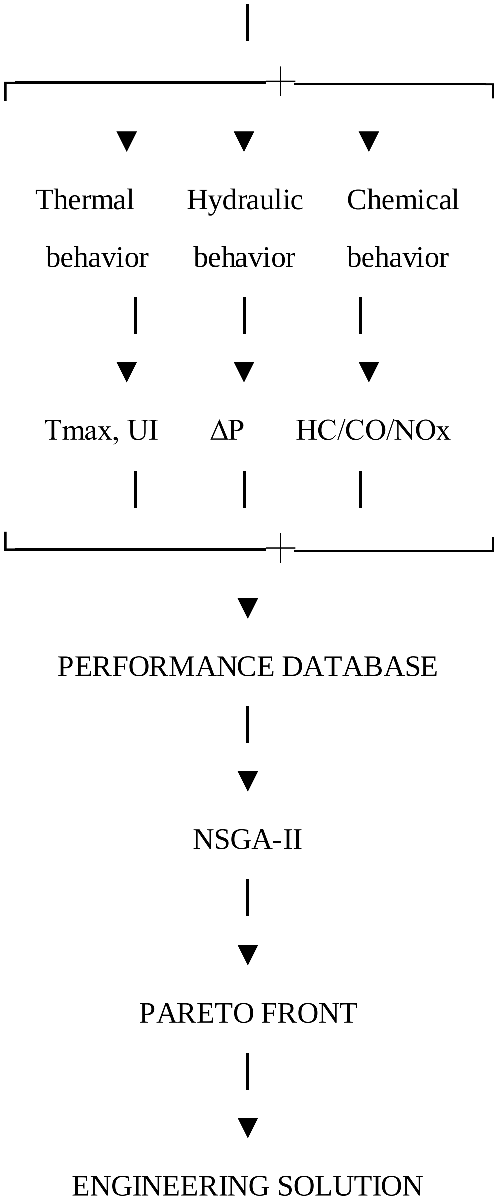

Figure 6. Proposed CFD–NSGA-II optimization framework for the flow-direction-transformed TWC.

---

31. Decision Variables and Optimization Bounds

Table 18. Optimization variables

Variable	Symbol	Investigated/reference values
Reversal time	τr	5–30 s
Inlet velocity	uin	1–6 m/s
Inlet temperature	Tin	CFD input

The International Journal of Engineering Sciences
https://international-journal-of-engineering-sciences.jo
Vol. 2, No. 1, 2026, pp. 25-53
ISSN 3104-8897

Air–fuel ratio	λ	Rich/lean
Porosity	ε	0.41 baseline
Washcoat thickness	δw	0.2 mm baseline

The numerical dataset provides explicit values for reversal time, velocity, porosity, and washcoat thickness. Additional CFD runs are required if optimization is extended beyond these baseline values.

32. Sensitivity Analysis

A normalized sensitivity coefficient can be expressed as:

$$S_x = \frac{\Delta\eta/\eta}{\Delta x/x}$$

The qualitative sensitivity ranking from the numerical results indicates that inlet velocity has a strong influence on HC and CO conversion.

The endpoint HC conversion changes by 28.2 percentage points between 1 and 6 m/s.

CO changes by 14.4 percentage points.

NOx exhibits a smaller 4.7 percentage-point change.

Table 19. Endpoint sensitivity

Response	1 m/s	6 m/s	Change
HC conversion	99.5%	71.3%	−28.2 pp
CO conversion	99.9%	85.5%	−14.4 pp
NOx conversion	85.7%	81.0%	−4.7 pp
Tmax	820 K	740 K	−80 K

HC is therefore particularly sensitive to the velocity-induced change in thermal and residence-time conditions.

33. Bangladesh-Oriented Engineering Interpretation

The Bangladesh application framework emphasizes operating situations characterized by variable vehicle speed and engine load.

The low-load condition is particularly important because low exhaust temperatures can reduce catalytic activity.

The flow-direction transformation approach provides a mechanism for retaining and redistributing thermal energy inside the catalyst.

The numerical results indicate that:

1. flow reversal improves HC conversion;
2. flow reversal improves CO conversion;
3. short reversal cycles can generate excessive transient disturbances;

4. reversal periods around 10–15 s provide a useful numerical operating window;
5. increasing velocity reduces residence time;
6. increasing velocity reduces maximum catalyst temperature;
7. reduced temperature and residence time decrease HC and CO conversion;
8. rich operation favors NOx conversion;
9. lean operation favors HC and CO oxidation; and
10. an integrated optimization strategy is required to balance these competing objectives.

34. Comparison with Conventional One-Way Operation

Table 20. Comparative performance

Criterion	One-way flow	Flow-direction transformation
HC conversion	84.6%	88.5–91.0%
CO conversion	94.7%	96.7–97.4%
Thermal regeneration	Limited	Enhanced
Thermal-zone redistribution	Limited	Stronger
Transient disturbance	Lower	Present
Actuation requirement	None	Required
Reversal-cycle optimization	Not applicable	Required

The flow-reversal design therefore introduces an operational-control requirement but provides measurable conversion improvements under the reference low-load condition.

35. Practical Design Implications

The findings suggest several design principles for flow-direction-transformed TWCs.

First, the reversal mechanism should not operate excessively rapidly because repeated switching produces transient periods during which pollutant conversion temporarily deteriorates.

Second, the catalyst should retain sufficient thermal mass to support regeneration after reversal.

Third, inlet velocity should be controlled within a range that provides sufficient residence time without creating excessive pressure loss.

Fourth, air–fuel management should account for the different requirements of oxidation and NOx reduction.

Fifth, catalyst design should balance active surface area against hydraulic resistance.

36. Limitations

Several limitations should be recognized.

ENGINEERING SCIENCE
The International Journal of Engineering Sciences
https://international-journal-of-engineering-sciences.jo
Vol. 2, No. 1, 2026, pp. 25-53
ISSN 3104-8897

First, the model represents hydrocarbons using C_3H_6 rather than a complete natural-gas hydrocarbon mixture. Methane-specific kinetics would be required for a dedicated methane-slip study.

Second, NOx is represented by NO, which simplifies the actual $NO/NO_2/N_2O$ distribution.

Third, particulate deposition and catalyst aging were neglected.

Fourth, catalyst poisoning and sulfur effects were not included.

Fifth, the walls were treated as adiabatic.

Sixth, the single-channel representation does not reproduce the full spatial distribution of a complete honeycomb monolith.

Seventh, pressure-drop values were not included in the available numerical data and were therefore excluded from the analysis rather than being estimated or artificially generated.

37. Recommended Extended CFD Campaign

For subsequent computational validation, the following simulation matrix is recommended.

Table 21. Proposed extended simulation matrix

Factor	Levels
Reversal time	5, 10, 15, 20, 25, 30 s
Velocity	1, 2, 3, 4, 5, 6 m/s
Load	Case 1–Case 4
Air–fuel condition	Rich / near-stoichiometric / lean
Catalyst porosity	Baseline + sensitivity range
Washcoat thickness	Baseline + sensitivity range
Output	HC, CO, NOx, Tmax, UI, ΔP

This matrix can subsequently be used to generate the complete Pareto front.

38. Principal Numerical Findings

Table 22. Consolidated numerical findings

Parameter	Numerical finding
One-way HC conversion	84.6%
Reversal HC conversion	88.5–91.0%
One-way CO conversion	94.7%
Reversal CO conversion	96.7–97.4%
Low-load HC conversion	88.5%
Low-load outlet HC	~0.08%
Approximate low-load reactor temperature	~800 K
Tmax at 1 m/s	~820 K
Tmax at 6 m/s	~740 K
HC conversion at 1 m/s	99.5%
HC conversion at 6 m/s	71.3%
CO conversion at 1 m/s	99.9%

CO conversion at 6 m/s	85.5%
NOx conversion at 1 m/s	85.7%
NOx conversion at 6 m/s	81.0%
Rich HC conversion	83.9%
Lean HC conversion	91.5%
Rich CO conversion	95.0%
Lean CO conversion	97.6%
Rich NOx conversion	96.3%
Lean NOx conversion	53.8%
Validation error	<5%
Recommended reversal window	10–15 s

39. Conclusions

This study developed a CFD-based numerical framework for evaluating a three-way catalytic converter incorporating periodic flow-direction transformation for natural-gas/diesel engine exhaust treatment in a Bangladesh-oriented application context.

The principal conclusions are as follows.

1. **Flow-direction transformation improves catalytic conversion.** Under the reference low-load condition, HC conversion increased from 84.6% under one-way flow to 88.5–91.0% under flow reversal. CO conversion increased from 94.7% to 96.7–97.4%.
2. **Thermal regeneration is a principal mechanism behind the improvement.** Reversal redistributes accumulated heat within the catalytic region and helps maintain catalyst activity during low-temperature operation.
3. **Reversal time strongly affects transient stability.** Excessively short reversal periods generate repeated transient deterioration. The original numerical results indicate that a reversal period in the approximate range of 10–15 s provides a useful operating window.
4. **Engine load affects catalytic thermal activity.** Even under the low-load reference case, the flow-reversal reactor approached approximately 800 K, while higher-load operation provided stronger thermal conditions and lower outlet HC concentrations.
5. **Inlet velocity is a major controlling variable.** Increasing velocity from 1 to 6 m/s reduced maximum reactor temperature from approximately 820 to 740 K and reduced HC conversion from 99.5% to 71.3%.
6. **CO conversion exhibits a similar velocity dependence.** CO conversion declined from 99.9% at 1 m/s to 85.5% at 6 m/s.
7. **NOx conversion is less sensitive to velocity than HC and CO within the reported endpoint conditions.** NOx conversion decreased from 85.7% to 81.0%.

ENGINEERING SCIENCE
The International Journal of Engineering Sciences
https://international-journal-of-engineering-sciences.jo
Vol. 2, No. 1, 2026, pp. 25-53
ISSN 3104-8897

8. **Air–fuel ratio produces a fundamental conversion trade-off.** Lean operation produced higher HC and CO conversion, whereas rich operation produced substantially higher NOx conversion.
9. **Residence time is directly linked to inlet velocity.** For the 200 mm catalytic section, residence time decreases from 0.20 s at 1 m/s to 0.0333 s at 6 m/s.
10. **Pressure drop must be considered alongside pollutant conversion.** A design that maximizes conversion without accounting for hydraulic resistance may impose an undesirable engine pumping penalty.
11. **Multi-objective optimization is therefore appropriate.** The proposed CFD–NSGA-II framework simultaneously considers HC, CO, NOx, thermal uniformity, and pressure drop.
12. **The framework provides a basis for Bangladesh-oriented catalyst design.** The numerical results can be used as the baseline dataset for subsequent CFD simulations involving local vehicle operating cycles, catalyst aging, methane-specific kinetics, and experimentally measured exhaust compositions.

Overall, the numerical evidence demonstrates that periodic flow-direction transformation provides a viable computational strategy for enhancing HC and CO conversion in catalytic converters operating under thermally challenging conditions. Its engineering implementation, however, requires simultaneous optimization of reversal timing, inlet velocity, air–fuel ratio, catalyst properties, thermal behavior, and pressure drop.

40. Data Availability Statement

The numerical data reported in this study were generated through the computational framework developed and implemented for the present investigation. The dataset includes the numerical results obtained from the CFD simulations, parametric analyses, and optimization procedures performed in this study. Additional CFD datasets generated during the study are available from the corresponding author upon reasonable request.

Ethical Considerations

Not applicable. This study did not require ethical approval because it does not include human or animal subjects and does not involve any personal or sensitive data.

List of Abbrevations:

(CFD): computational fluid dynamics; (TWC): Three-way catalytic converter; (HC): hydrocarbons ,(CO): carbon monoxide , (NOx): nitrogen oxides; FDT: Flow-direction transformation; τr: Reversal time;

Acknowledgment:

The authors would like to express their sincere gratitude to the **Department of Mechanical Engineering, Chittagong University of Engineering and Technology, Chattogram 4349, Bangladesh**, for its academic and institutional support. The authors also gratefully acknowledge the partial research funding provided to support the conduct of this study under **Grant No. **BANGLADESH.2026.MECH.CHITTAGONO.UNIVERSITY44521SDK8****.

The authors further express their sincere gratitude to **The International Journal of Engineering Sciences – Noor Al-Ilm for Publishing and Distribution** for its generous support in waiving all publication fees and facilitating the publication of this manuscript free of charge. This publication fee waiver was provided as editorial and publication support and did not involve any influence on the study design, data collection, computational analysis, interpretation of results, or reporting of the research. The authors highly appreciate the journal's commitment to promoting scientific research and supporting researchers.

Author Contribution:

All authors contributed equally to the main contributor to this paper. All authors read and approved the final paper.

Declaration of generative AI and AI-assisted technologies in the writing process

The authors hereby declare that no generative artificial intelligence or AI-assisted technologies were used at any stage during the preparation of this manuscript, including language editing, proofreading, or content development. The authors take full responsibility for the originality and integrity of the work presented in this publication.

The International Journal of Engineering Sciences
https://international-journal-of-engineering-sciences.jo
Vol. 2, No. 1, 2026, pp. 25-53
ISSN 3104-8897

Funding:

This research received partial financial support under **Grant No. BANGLADESH.2026.MECH.CHITTAGONO.UNIVERSITY44521SDK8**, provided to support the conduct of the study. The authors also acknowledge **The International Journal of Engineering Sciences, Noor Al-Ilm for Publishing and Distribution**, for providing a full waiver of the publication fees. The publication fee waiver was provided as editorial and publication support and did not involve any financial contribution to, or influence on, the conduct, design, computational analysis, interpretation, or reporting of the research.

Conflicts of Interest:

"The authors declare no conflict of interest."

References

[1] Bajwa, A. U., & Sheikh, H. A. (2023). Contribution of Road Transport to Pakistan's Air Pollution in the Urban Environment. Air, 1(4), 237-257. https://doi.org/10.3390/air1040018

[2] Joshi, A., "Review of Vehicle Engine Efficiency and Emissions," SAE Int. J. Adv. & Curr. Prac. in Mobility 4(5):1704-1733, 2022, https://doi.org/10.4271/2022-01-0540

[3] Fattah, M. A., Esraz-Ul-Zannat, M., Morshed, S. R., & Roni, A. T. (2022). Modeling the impact of motorized vehicles' activities on emissions and economic losses in a fast-growing developing city, Dhaka, Bangladesh. Journal of Transport & Health, 25, 101377. https://doi.org/10.1016/j.jth.2022.101377

[4] Петришин, І., Середюк, Д., Бас, О., & Мануляк, Р. (2022). Aspects of the introduction of alternative gas fuels and their influence on the quality of natural gas. Український метрологічний журнал/Ukrainian Metrological Journal, (2), 52-57. DOI: https://doi.org/10.24027/2306-7039.2.2022.263892

[5] Dilsher Khan, Geetesh Goga,2023. A review on performance and emission characteristics of a diesel engine fueled with gaseous & liquid fuels, Materials Today: Proceedings, Volume 80, Part 1, 2023, Pages A14-A22, ISSN 2214-7853, https://doi.org/10.1016/j.matpr.2023.04.197

[6] Liu, J., Zhao, W., Zhang, X., Ji, Q., Ma, H., Sun, P., & Wang, P. (2024). Optimizing combustion and emissions in natural gas/diesel dual-fuel engine with pilot injection strategy. Thermal Science and Engineering Progress, 48, 102418. https://doi.org/10.1016/j.tsep.2024.102418

[7] Jin, N., Long, W., Xie, C., & Tian, H. (2025). After-Treatment Technologies for Emissions of Low-Carbon Fuel Internal Combustion Engines: Current Status and Prospects. Energies, 18(15), 4063. https://doi.org/10.3390/en18154063

[8] Wang, W., Mai, Z., Yao, X., Tang, C., & Huang, Z. (2024). Towards optimized excess air ratio and substitution rate for a dual fuel HPDI engine. Applied Thermal Engineering, 253, 123797. https://doi.org/10.1016/j.applthermaleng.2024.123797

[9] Tripathi G and Dhar A (2022) Performance, emissions, and combustion characteristics of methane-diesel dual-fuel engines: A review. Front. Therm. Eng. 2:870077. doi: https://doi.org/10.3389/fther.2022.870077

[10] García A, Pastor JV, Monsalve-Serrano J, Fogué-Robles Á. Engine-out hydrocarbon speciation and DOC reaction modeling for dual-fuel combustion concept. International Journal of Engine Research. 2024;25(11):2088-2107. doi: https://doi.org/10.1177/14680874241262048

[11] Malfi E, Esposito S, De Felice M, Pitsch H, Pischinger S, De Bellis V. Phenomenological model for unburned hydrocarbon emissions from spark-ignition, pre-chamber, and dual-fuel internal combustion engines. International Journal of Engine Research. 2024;25(10):1818-1834. doi: https://doi.org/10.1177/14680874241255157

[12] Jena, S., & Padhy, M. (2025). The Environment and Catalytic Converter—A Review. Mater. Int, 7(7). 7 https://doi.org/10.33263/Materials71.007

[13] Li, P., Li, Q., Sun, X., Zhang, G., Jiang, Y., Zheng, C., & Yang, Z. (2025). Energy-saving elimination of CO and NOx via self-sustained reaction coupling in layered monolithic catalysts. Separation and Purification Technology, 135756. https://doi.org/10.1016/j.seppur.2025.135756

[14] Robles-Lorite, L., Dorado-Vicente, R., Torres-Jiménez, E., Bombek, G., & Lešnik, L. (2023). Recent Advances in the Development of Automotive Catalytic Converters: A Systematic Review. Energies, 16(18), 6425. https://doi.org/10.3390/en16186425

[15] Desouky, O. (2022). Integration of Engine and TWC Models through Developing an Exhaust Manifold Model for Predicting Motor Vehicle Emissions during Drive Cycles (Doctoral dissertation). https://oaktrust.library.tamu.edu/items/ede9ad78-c747-4918-a8ab-81b59a14cdc7

[16] Zazhigalov, S., Elyshev, A., & Zagoruiko, A. (2023). Catalytic reverse-flow oxidation process in reactors of various designs: Axial, side and tangential gas inlet. Chemical Engineering Research and Design, 191, 364-374. https://doi.org/10.1016/j.cherd.2023.01.045

[17] Gai, C., Tao, Y., Peng, N., Dou, X., & Liu, Z. (2025). Sustainable regeneration of deactivated hydrochar-supported Ni catalyst for enhancing low-temperature tar reforming performance. Journal of Analytical and Applied Pyrolysis, 186, 106918. https://doi.org/10.1016/j.jaap.2024.106918

[18] Elahe Pourghadiri, Ataallah Sari; Theoretical Investigation on Syngas Production by Catalytic Partial Oxidation of Methane in a Reverse-Flow Microchannel Monolithic Reactor. Ind. Eng. Chem. Res. 21 June 2023; 62 (24): 9433–9452. https://doi.org/10.1021/acs.iecr.3c00594

[19] Beg, M. B., Ali, L., Nambyaruveettil, S., Jawed, A. S., & Altarawneh, M. (2025). Dual low-temperature simultaneous catalytic combustion of methane and carbon monoxide in relevance to combating emission from natural gas vehicles (NGVs). Energy, 139006. https://doi.org/10.1016/j.energy.2025.139006

[20] Bae, W. B., Byun, S. W., Hazlett, M., Yoon, D. Y., Jung, C., Kim, C. H., & Kang, S. B. (2022). Emission of NH3 and N2O during NO reduction over commercial aged three-way catalyst (TWC): Role of individual reductants in simulated exhausts. Chemical Engineering Journal Advances, 9, 100222. https://doi.org/10.1016/j.ceja.2021.100222

[21] Xu, X., Liu, W., Wang, Y., Cheng, Q., Wang, Q., Li, Z., & Qi, J. (2026). Enhancing Thermal Uniformity and Ventilation Air Methane Conversion in Pilot-Scale Regenerative Catalytic Oxidizers via CFD-Guided Structural Optimization. Catalysts, 16(1), 38. https://doi.org/10.3390/catal16010038

The International Journal of Engineering Sciences
https://international-journal-of-engineering-sciences.jo
Vol. 2, No. 1, 2026, pp. 25-53
ISSN 3104-8897

[22] Patel, K. D., Subedar, D., & Patel, F. (2022). Design and development of automotive catalytic converter using non-nobel catalyst for the reduction of exhaust emission: A review. Materials Today: Proceedings, 57, 2465-2472. https://doi.org/10.1016/j.matpr.2022.03.350

Authors and Affiliations

Nizam S. Wafeeq, [1a,*] R. S. Rahman;[1b] Adib D. Ali;[1c] Jamal Uddin Sadiq;[1d] Hassan T. Karim;[1e] E.B. Kabir;[1f] Ari Y. Rassool;[1g] Zeinuldeen U. Baker;[1h] Mohammed R. Shaheed;[1j] Muslim Y.Q. Meraz;[1k]

[1] Department of Mechanical Engineering, Chittagong University of Engineering and Technology, Chattogram, 4349, Bangladesh.

Nizam.waf.47@cuet.ac.bd [a]	r.s..rahman87@cuet.ac.bd ,[b]
adib.d.ali@cuet.ac.bd [c]	jamaluddin.sad5@cuet.ac.bd d
hasan.t.karim@cuet.ac.bd ,[e]	e.b.kabir1986@cuet.ac.bd ,[F]
ari_rasool@cuet.ac.bd g	zeinuldeen_baker@cuet.ac.bd h
r.shaheed4895@cuet.ac.bd i	y.q.meraz@cuet.ac.bd j

*** Corresponding Author**: Nizam S. Wafeeq *, Nizam.waf.47@cuet.ac.bd